

## Isotope shifts and hyperfine structure of the $4s^2\ ^1S_0$ - $4s\ 4p\ ^1P_1$ transition in calcium isotopes

A. Andl, K. Bekk, S. Göring, A. Hanser, G. Nowicki, H. Rebel, G. Schatz, and R. C. Thompson

*Kernforschungszentrum Karlsruhe GmbH, Institut für Angewandte Kernphysik,*

*D-7500 Karlsruhe, Federal Republic of Germany*

(Received 6 May 1982)

Isotope shifts and hyperfine structure splittings of the CaI resonance line ( $4s^2\ ^1S_0$ - $4s\ 4p\ ^1P_1$ ,  $\lambda=422.7$  nm) have been measured for all calcium isotopes between  $^{40}\text{Ca}$  and  $^{48}\text{Ca}$ , including the short-lived isotope  $^{47}\text{Ca}$  ( $T_{1/2}=4.54$  d). Resonance fluorescence was observed in a well-collimated atomic beam of calcium excited by a narrow band tunable continuous-wave dye laser. Combining the result with muonic x-ray data for the stable isotopes, accurate values for the changes of mean square charge radii of the Ca nuclei are obtained, in addition to information on electromagnetic moments from the measured hyperfine structure constants. The influence of ground state correlations (represented by quadrupole and octupole mean square deformations) on the observed peculiar variation of the Ca charge radii is discussed as well as the relation to the droplet model and to a mixed  $(f_{7/2})^n$  model.

[ NUCLEAR STRUCTURE Isotope shifts and hyperfine structure of  
Ca isotopes,  $A=40$  to  $48$ , measured by laser spectroscopy, deduced  
 $\delta\langle r^2 \rangle$  and nuclear moments. ]

### I. INTRODUCTION

For many reasons information on isotope shifts and hyperfine interactions for Ca isotopes is of great interest. The nuclides  $^{40}\text{Ca}$  and  $^{48}\text{Ca}$  are both doubly magic and studies of the size and shape of the nuclei in the series of Ca isotopes yield information on interesting effects associated with the addition of neutrons in the  $f_{7/2}$  shell. Consequently, there are considerable theoretical and experimental activities investigating charge and matter distributions of Ca nuclei by many different methods.<sup>1</sup> There is also a long tradition of measuring optical isotope shifts which have long been a valuable tool for precise and detailed investigations (see Ref. 2 for a compilation of experiments with Ca isotopes). Recently, by use of high resolution laser spectroscopy combined with highly sensitive methods of detection, the experiments could be extended to radioactive nuclei<sup>3</sup> and these laser methods are, in fact, the only techniques applicable to the small amounts of radioactive material. In a series of investigations<sup>4</sup> the Heidelberg group has applied high-resolution intracavity spectroscopy to observing the very weak intercombination line 657.3 nm ( $4s^2\ ^1S_0 \rightarrow 4s\ 4p\ ^3P_1$ ). Although this line has the advantage of a very small natural line width (410 Hz) and of a convenient spectral range for tunable

continuous-wave (cw) dye lasers, the sensitivity of the technique remains restricted to radioactive samples in the range of  $10\ \mu\text{g}$ , and it is therefore not feasible for  $^{47}\text{Ca}$  ( $T_{1/2}=4.5$  d), for which only sub-nanogram samples can conveniently be produced.

In this paper we report on high resolution laser spectroscopic measurements of isotope shifts and hyperfine structure splittings of the blue  $4s^2\ ^1S_0$ - $4s\ 4p\ ^1P_1$  resonance transition in all Ca isotopes between  $^{40}\text{Ca}$  and  $^{48}\text{Ca}$ , including  $^{47}\text{Ca}$ , measured for the first time. (The results have already been briefly reported in Refs. 5 and 6.) The experimental technique applied makes use of isotope selective excitation in a well collimated atomic beam intersected by the light beam of a stabilized cw dye laser and detection of the emitted resonance fluorescence light. The combination of the results with muonic x-ray data<sup>7</sup> then yields highly accurate values for the variation of the mean square nuclear charge radii in the chain of Ca isotopes. The radius difference  $\delta\langle r^2 \rangle_{47-40}$  proves to be very small and fits well into the known peculiar variation of the Ca charge radii. Values of  $A$  and  $B$  factors of hyperfine splitting observed in odd Ca isotopes are additionally given. We find a discrepancy between the  $B$  factor ratios deduced for the  $^3P_0$  state and those for the  $^3P_1$  state, which might be an indication of a strong influence of second order corrections.<sup>8</sup>

## II. EXPERIMENTS

### A. Experimental method

Laser induced atomic beam fluorescence spectroscopy has been applied successfully in our laboratory to the investigation of stable and radioactive Ba nuclides<sup>9,10</sup> and provides the necessary resolution and sensitivity in the case of calcium as well. The calcium  $4s^2\ ^1S_0-4s\ 4p\ ^1P_1$  resonance transition ( $\lambda=422.7$  nm) was excited by jet-stream dye lasers operating with stilbene 3 dye and pumped by the uv lines of an argon ion laser. One laser, built in the laboratory,<sup>6</sup> was locked to the resonance frequency of  $^{40}\text{Ca}$  in an atomic beam, thus providing an optical reference frequency. The output of a second laser (Coherent Radiation model 599-21) crossed a separate, highly collimated atomic beam containing the Ca isotopes to be studied. Part of the output was also mixed with that of the first laser on a fast photodiode. The difference frequency was locked to a value which was then scanned under computer control during the recording of a spectrum. In order to be able to cover the whole of the spectral profile of  $^{40}\text{Ca}$  (where the difference frequency would otherwise pass through zero), the frequency of the reference laser was shifted by 250 MHz before mixing, using an acousto-optic modulator. Further details of the experimental procedures, frequency stabilization of the lasers, and atomic beam apparatus can be found in Refs. 6 and 10.

The total fluorescence spectrum (from  $^{40}\text{Ca}$  to  $^{48}\text{Ca}$ ) covers a range of approximately 1.6 GHz. A laser power of typically 0.05 mW was used for the measurements. At higher power, optical pumping effects set in for the odd isotopes. Spectra were recorded with laser light linearly polarized either parallel or perpendicular to the observation direction.

In most spectra the observed linewidth was 42 MHz (FWHM) to be compared to the natural width of 35 MHz. With samples of typically 10 ng per isotope the count rates were of the order of 100 kHz in the peaks. Interference terms for the odd isotopes were included in the computer analysis of the measured fluorescence spectra.

As the available  $^{47}\text{Ca}$  sample was smaller, the measuring method was slightly modified in order to avoid optical pumping effects. A Pockels cell driven by a radio-frequency (rf) oscillator was inserted in the laser beam such that the laser light polarization was continuously modulated between parallel and perpendicular to the observation direc-

tion, at a rate of 5 MHz. This allows an increase of the laser power as there is not enough time for the atoms to get optically pumped before the polarization changes. This modulation introduces side bands of appreciable intensity at  $\pm 5$  and  $\pm 10$  MHz, but the resulting broadening of the fluorescence lines is not a serious problem. Using this method, fluorescence spectra for  $^{47}\text{Ca}$  (Fig. 1) were obtained with a laser power of 0.5 mW without any detectable optical pumping effects.

### B. Sample preparation

The natural abundances of the six stable calcium isotopes differ by more than four orders of magnitude. In order to produce samples containing approximately equal amounts of each of the stable isotopes or to separate target material from a radioactive Ca nuclide produced by irradiation, an electromagnetic mass separator<sup>11</sup> was used. The radioactive isotopes  $^{41}\text{Ca}$ ,  $^{45}\text{Ca}$ , and  $^{47}\text{Ca}$  were all produced by neutron capture in enriched Ca samples irradiated in the Karlsruhe research reactor FR 2.

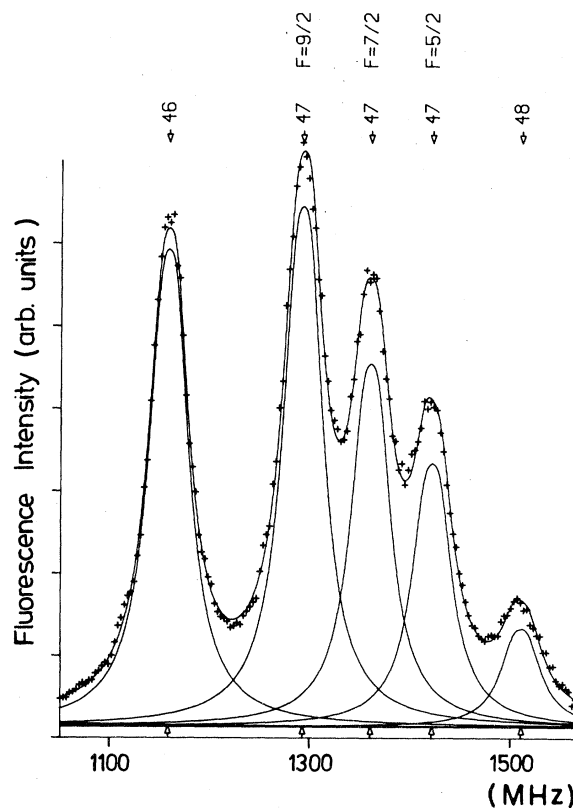


FIG. 1. Spectrum of a  $^{46-48}\text{Ca}$  sample containing only  $\sim 170$  pg  $^{47}\text{Ca}$ .

The ion beam from the mass separator implanted the desired isotope directly into the tantalum oven, then used in the atomic beam apparatus. Contamination caused by naturally occurring calcium could be eliminated by preheating the oven under high vacuum.

$^{41}\text{Ca}$  ( $T_{1/2}=1.3\times 10^5 a$ ) was produced from a 3 mg sample of natural CaO. After irradiating this target for  $1\frac{1}{2}$  yr with a neutron flux of about  $9\times 10^{13} n \text{ cm}^{-2} \text{ s}^{-1}$ , 18 ng of  $^{41}\text{Ca}$  were obtained in the atomic beam oven following mass separation. A sample containing 5 ng of  $^{45}\text{Ca}$  ( $T_{1/2}=163 \text{ d}$ ) was produced in the same way from 1 mg of CaO with  $^{44}\text{Ca}$  isotopically enriched to 95%.  $^{47}\text{Ca}$  ( $T_{1/2}=4.5 \text{ d}$ ) was obtained from a target consisting of 2 mg of  $\text{CaO}_3$  enriched to 43%  $^{46}\text{Ca}$ . After 14 d of irradiation with  $9\times 10^{13} n \text{ cm}^{-2} \text{ s}^{-1}$  followed by mass separation, 170 pg of  $^{47}\text{Ca}$  were available in the atomic beam oven.

$^{41}\text{Ca}$  and  $^{45}\text{Ca}$  were implanted in the same oven, so that they could be measured in the same run. Similar quantities of  $^{40}\text{Ca}$ ,  $^{44}\text{Ca}$ , and  $^{48}\text{Ca}$  were added to provide reference points in the scan. Similarly,  $^{46}\text{Ca}$  and  $^{48}\text{Ca}$  were added to the  $^{47}\text{Ca}$  sample. More than one sample was produced for each isotope, and we were able to measure a number of spectra from each sample, thus checking the internal consistency of the measurements and the reproducibility of the results.

An attempt was also made to measure  $^{49}\text{Ca}$  ( $T_{1/2}=8.7 \text{ min}$ ). A sample containing approximately 1 pg was prepared by neutron capture on enriched  $^{48}\text{Ca}$ . In spite of a mass separation, a much larger amount of  $^{48}\text{Ca}$  was present in the atomic beam. The photon burst method developed by Greenlees *et al.*<sup>35</sup> was used in order to suppress the

long Lorentzian tail of the  $^{48}\text{Ca}$  resonance line. No resonance attributable to  $^{49}\text{Ca}$  was found. From a careful analysis of the observed  $^{48}\text{Ca}$  line and as  $^{49}\text{Ca}$  was there in the expected amount, we may conclude that the shift between these two isotopes is rather small:

$$\Delta\nu^{49-48} \leq 50 \text{ (MHz)} .$$

### III. RESULTS

#### A. Isotope shifts and nuclear radii

Table I presents the measured isotopic shifts for all isotopes between  $A=40$  and 48. The values for the stable isotopes are compared to the results of Brand *et al.*<sup>12</sup> for the same transition. Satisfactory agreement is found. A King plot with the results<sup>4</sup> for the intercombination line  $^1S_0-^3P_1$  ( $\lambda=657.3 \text{ nm}$ ) is displayed in Fig. 2. Seven of the eight data points are located on a straight line within their respective errors showing that these sets of data are well consistent. This is not the case for  $^{41}\text{Ca}$ , where a clear discrepancy (by about two standard deviations) exists.

The measured isotope shifts  $\delta\nu_i^{AA'}$  of a particular optical transition ( $i$ ) are the sum of a shift  $\delta\nu_{\text{mass}}$  due to the change in mass of the nucleus and of a shift resulting from the variation of the nuclear charge radius

$$\delta\nu_i^{AA'} = M_i \left[ \frac{1}{A'} - \frac{1}{A} \right] + F_i \delta \langle r^2 \rangle^{AA'} . \quad (3.1)$$

TABLE I. Measured isotopic shifts  $\delta\nu(A-40)$  of the  $4s^2\ ^1S_0-4s\ 4p\ ^1P_1$  resonance transition ( $\lambda=422.7 \text{ nm}$ ) and derived differences of the mean square nuclear charge radii  $\delta \langle r^2 \rangle$ . The optical values  $\delta \langle r^2 \rangle$  use for calibration results from muonic x-ray data and are therefore not independent of these.

Atomic number $A$	Isotopic shifts $\delta\nu$ (MHz)		Mean square radii differences ( $\text{fm}^2$ )	
	This work	Brandt <i>et al.</i> <sup>a</sup>	From muonic x rays <sup>b</sup>	This work
41	223.2(12)			-0.012(7)
42	391.1(8)	389.4(30)	0.215(11)	0.221(12)
43	611.0(10)	607.8(30)	0.116(24)	0.117(6)
44	770.8(8)	772.8(30)	0.298(9)	0.293(12)
45	983.9(18)			0.128(20)
46	1158.9(8)	1164.6(36)	0.164(43)	0.128(8)
47	1348.7(12)			0.007(10)
48	1510.7(8)	1507.5(30)	-0.001(6)	0.000(9)

<sup>a</sup>Reference 12.

<sup>b</sup>Table II of Ref. 7.

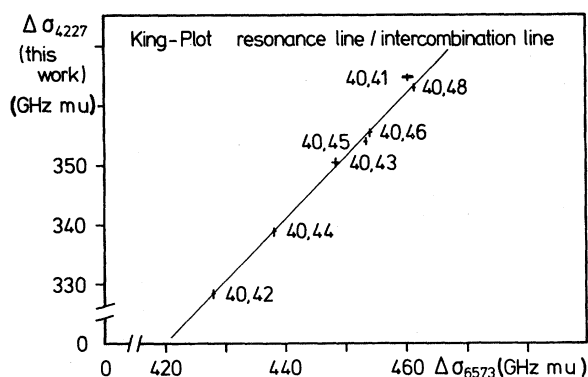


FIG. 2. King diagram with the isotope shifts of the CaI intercombination line  $^1S_0-^3P_1$  ( $\Delta\sigma = A'A / (A' - A) \times \delta\nu$ ).

For light nuclei, the mass effect dominates, and the volume effect and nuclear structure effects contribute as a rule less than 10% of the total shift.  $F_i$  and  $M_i$  are quantities determined by the atomic structure and need to be known if  $\delta\langle r^2 \rangle$  values are to be extracted. As values of  $\delta\langle r^2 \rangle$  for the stable Ca isotopes are known from electron scattering and muonic x-ray studies,<sup>7</sup> it is possible to determine  $M_i$  and  $F_i$  experimentally. A King plot with the muonic x-ray data (Fig. 3) demonstrates that the linear relationship between  $\delta\nu_i$  and  $\delta\langle r^2 \rangle$  holds within the accuracy of the measurements. The results are the following:

$$M_i(\lambda = 422.7 \text{ nm}) = 362.54(44) \text{ (GHz mu)},$$

$$F_i(\lambda = 422.7 \text{ nm}) = -181(10) \text{ (MHz fm}^{-2}\text{)}.$$

With the known values of  $M_i$  and  $F_i$  we calculate the mean square (ms) charge radii differences of the unstable isotopes  $^{41,45,47}\text{Ca}$  and improve the accuracy of the (comparatively imprecise) muonic x-ray

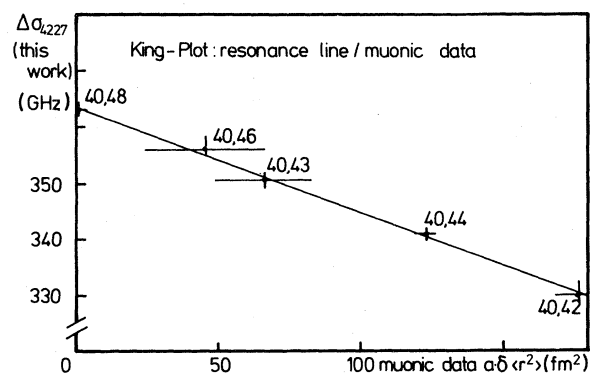


FIG. 3. King diagram using muonic x-ray result from Ref. 7 ( $\Delta\sigma = A'A / (A' - A) \times \delta\nu$ ).

data for the isotopes  $^{43,46}\text{Ca}$ . The results are given in the last column of Table I. We note that the muonic x-ray shifts are primarily due to a different type of moment (Barret radii) and that the conversion into equivalent root-mean-square (rms) radii is not completely model independent.

The mass shift of the isotope shift is traditionally split up into the normal mass shift (NMS)

$$[M_i(\text{normal}) = \nu_i / 1822]$$

which is the familiar reduced mass correction, and the specific mass shift (SMS), which is due to  $\langle \vec{p}_j \cdot \vec{p}_k \rangle$  correlation terms of the electron momenta and is not easily calculated. The calibration by help of the muonic x-ray results allows us to determine the SMS part,

$$\text{SMS/NMS} = -0.069(1).$$

It proves to be very small, as expected for an  $ns^2$ - $nsnp$  optical transition.<sup>13</sup>

In a simple nonrelativistic approximation (see Ref. 6) the coefficient

$$F_i = -\frac{Ze^2 \Delta\rho_i(0)}{6h\epsilon_0} \text{ (Hz m}^{-2}\text{)} \quad (3.2)$$

is essentially determined by the change of the electron density  $\Delta\rho_i$  ( $\text{m}^{-3}$ ) at the nuclear site during the atomic transition. We find experimentally

$$\Delta\rho_i = 12.4(7) \text{ (\AA}^{-3}\text{)}.$$

For  $^{49}\text{Ca}$  we conclude from the upper limit of the isotope shift quoted in Sec. II B that the radius difference between  $^{48}\text{Ca}$  and  $^{49}\text{Ca}$  is rather large ( $\delta\langle r^2 \rangle \geq 0.5 \text{ fm}^2$ ). This comparatively large jump is not unexpected since a large increase in radius has been observed in many cases at the beginning of a neutron shell.

## B. Nuclear moments

Table II gives the  $A$  and  $B$  factors calculated from the hyperfine splittings of the transition frequencies for the four odd isotopes. The values for  $^{43}\text{Ca}$ , the only stable odd isotope, are in good agreement with results of a level crossing experiment.<sup>14</sup> In Table III hyperfine structure (hfs) constants relative to the value for  $^{43}\text{Ca}$  are presented and compared to the corresponding ratios obtained for the  $4s4p^3P_1$  level using laser and combined laser rf spectroscopy.<sup>4</sup> Corresponding  $A$  factor ratios are in good agreement for the two transitions. Using the well known value<sup>14</sup> for the magnetic moment of

TABLE II. Measured  $A$  and  $B$  factors of the  $^1P_1$  state hyperfine structure for the odd Ca isotopes.

Isotope	$A$ (MHz)	$B$ (MHz)
41	-18.84(13)	-9.2(6)
43	-15.46(15)	-9.7(7)
45	-15.45(12)	+1.8(5)
47	-16.20(23)	+4.1(6)

$^{43}\text{Ca}$  [ $\mu = 1.2172(6) \mu_N$ ] as normalization and neglecting any hyperfine anomaly, the magnetic moments given in Table III are derived.

The relatively small  $B$  factor values reflect small values of the nuclear quadrupole moments. In such a case, it appears to be somewhat dangerous to apply the usual formula relating the  $B$  factor

$$B = \frac{2}{3} \frac{e^2}{hc} Q_{\text{hfs}} \langle r_e^{-3} \rangle R_r (\text{cm}^{-1}) \quad (3.3)$$

to the spectroscopic quadrupole moment via  $\langle r_e^{-3} \rangle$  values [taken from *ab initio* calculations or deduced from atomic data<sup>15</sup> with a relativistic correction  $R_r$  (Ref. 15) and an additional antishielding factor due to the Sternheimer effect<sup>16</sup>]. Such a first order result does not include polarization and correlation effects which have been shown to be occasionally important.<sup>8</sup> Estimating these effects, Grundevik *et al.*<sup>18</sup> deduce a value for the quadrupole moment  $Q(^{43}\text{Ca}) = -0.065(20)$  (e b) [this value agrees well with a recently reported result<sup>19</sup>  $Q = -0.062(12)$  (e b)] from the value

$$B(^3P_2) = -5.436(8) \text{ MHz},$$

precisely measured for the  $4s 4p ^3P_3$  metastable state of  $^{43}\text{Ca}$ . As seen in Table III, the  $B$  factor ratios found in our experiments deviate severely from

those obtained for the  $^3P_1$  state. For the ratio  $B(^{41}\text{Ca})/B(^{43}\text{Ca})$ , the discrepancy is of the order of 30%, for which higher order effects might be responsible. But we find it difficult to believe that this could also explain the large difference in the  $B(^{45}\text{Ca})/B(^{43}\text{Ca})$  ratios. In view of this discrepancy (and before second order corrections have been calculated), we therefore prefer not to quote any values of the nuclear quadrupole moments.

#### IV. DISCUSSION

The normal variation expected for the ms radius of nuclear charge distributions is an increase with the mass number  $A$ . Figure 4 displays the peculiar behavior of the Ca isotopes showing a decrease of  $\langle r^2 \rangle$  when filling up the second half of the neutron shell at  $N=28$ . The following features emerge from Fig. 4:

(i) The rms charge radii of  $^{40}\text{Ca}$  and  $^{48}\text{Ca}$  are equal within experimental uncertainty, whereas the even nuclei in between have a charge radius larger in size by about 1%.

(ii) There is a distinct odd-even staggering. The odd  $^{43}\text{Ca}$  nucleus is considerably smaller than its neighbors as far as the charge distribution is concerned.

(iii) There is only a minute difference (if any) between the charge radii of  $^{40}\text{Ca}$  and  $^{41}\text{Ca}$ .

There is a striking similarity<sup>2,3</sup> between the variation of the ms charge radii and the trends of the quadrupole transition strengths inferred from inelastic  $\alpha$ -particle scattering,<sup>20</sup>  $B(E2)$  values of the lowest  $2^+$  states, and transition radii measured for the  $0_1^+ \rightarrow 0_2^+$  monopole transitions by inelastic electron scattering<sup>21</sup> (Fig. 5). This similarity suggests

TABLE III.  $A$  and  $B$  factors for the two states  $^1P_1$  and  $^3P_1$  normalized to the respective values for  $^{43}\text{Ca}$ . The last column gives the nuclear magnetic moments  $\mu$ , calculated from the known value for  $^{43}\text{Ca}$  using the ratios of the  $A$  factors from our data, thus neglecting any hyperfine anomaly.

Isotope	$^1P_1$ state (this work)		$^3P_1$ state		Magnetic moment ( $\mu_N$ )
	$A/A(^{43}\text{Ca})$	$B/B(^{43}\text{Ca})$	$A/A(^{43}\text{Ca})$	$B/B(^{43}\text{Ca})$	
41	1.219(15)	0.95(9)	1.210 242(21) <sup>a</sup>	1.647(6) <sup>a</sup>	-1.606(20)
43	1.000	1.00	1.000 000	1.0000	-1.3172(6) <sup>c</sup>
45	0.999(12)	-0.19(5)	1.0076(5) <sup>b</sup>	-1.22(30) <sup>b</sup>	-1.316(16)
47	1.048(18)	-0.42(7)			-1.380(24)

<sup>a</sup>From Ref. 17.

<sup>b</sup>From Ref. 4.

<sup>c</sup>From Ref. 14.

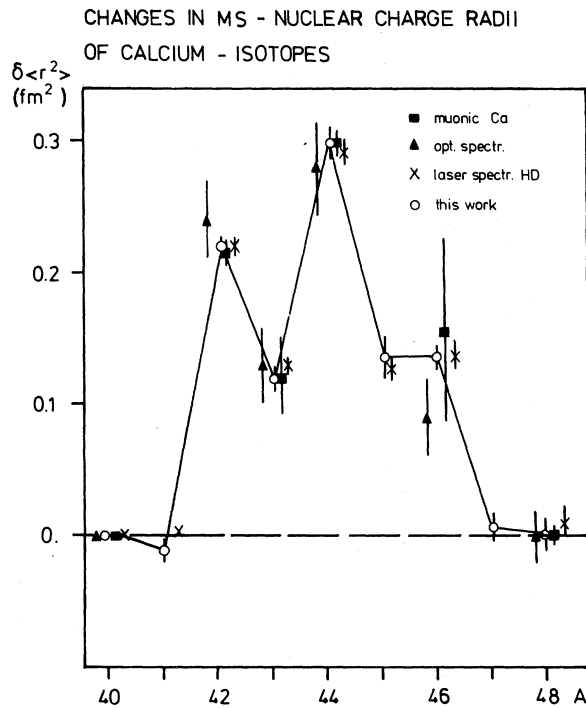


FIG. 4. Variation of the mean square nuclear charge radii of the Ca isotopes.

an explanation based on fluctuations of the long range ground state correlations phenomenologically represented by the ms deformation  $\langle \beta^2 \rangle$ .

Splitting up

$$\delta \langle r^2 \rangle = \delta \langle r^2 \rangle_0 + \frac{5}{4\pi} \langle r^2 \rangle_0 \delta \langle \beta_L^2 \rangle \quad (4.1)$$

into a monopole part and a deformation effect  $\delta \langle \beta_L^2 \rangle$  and introducing experimental  $\delta \langle \beta_2^2 \rangle$  values derived from measured  $B(E2, 0^+ \rightarrow 2_1^+)$  values,<sup>22,23</sup> we find indeed the major part of the variation of the even Ca nuclei to be attributable to the variation of the quadrupole deformation and  $\delta \langle r^2 \rangle_0 \cong 0$ . This explanation (see Ref. 3) tacitly assumes that the strongest effects result only from the  $B(E2)$  values of the first  $2^+$  states and that contributions from giant resonances<sup>24</sup> and higher multipolarities give rise merely to a smooth and negligible background. However, Ca isotopes also show pronounced fluctuations of the octupole strength. A marked development from a strong  $3_1^-$  state in  $^{40}\text{Ca}$  towards a weak one in  $^{48}\text{Ca}$  is observed.<sup>23</sup> Moreover, electron scattering experiments (see Ref. 1) have shown that the skin thickness of the charge distribution of  $^{48}\text{Ca}$  is considerably smaller than for the  $^{40}\text{Ca}$  nucleus. These findings should be con-

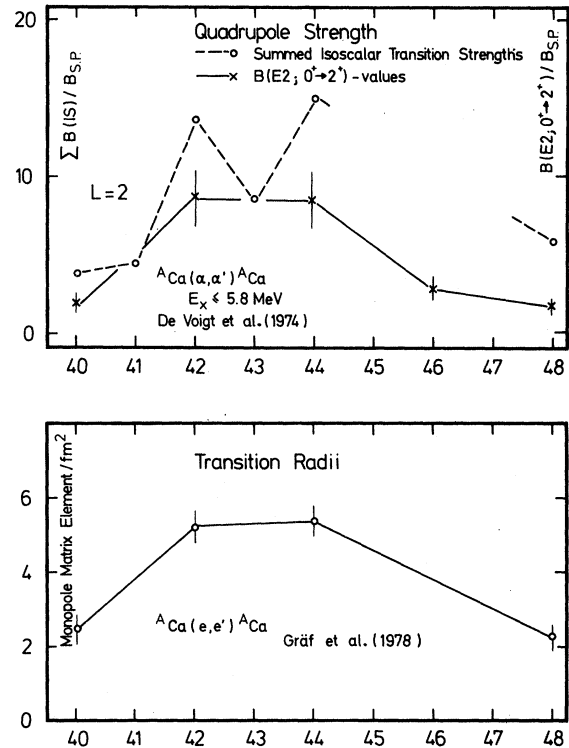


FIG. 5. Trends of  $E2$  strengths and transition radii of the Ca isotopes.

sistently included into the consideration of deformation effects.

Recently, Friedrich and Voegler<sup>25</sup> systematically analyzed elastic electron scattering form factors on the basis of a convenient parametrization (Helm's model<sup>26</sup>) of the nuclear charge distribution. This parametrization folds a homogeneously charged sphere (with radius  $R$ ) with a Gaussian of variance  $\sigma$

$$\rho(r) = \int \rho_{\text{h.s.}}(\vec{r}; R) \cdot \rho_G(\vec{r} - \vec{r}', \sigma) d^3 r'. \quad (4.2)$$

The parameter  $\sigma$  is rather accurately related to the skin thickness  $t$  and the diffuseness  $a$  of a Fermi distribution by

$$t = 2.54\sigma = 4.39a. \quad (4.3)$$

Friedrich and Voegler<sup>25</sup> have shown that the extension parameter  $R$  is identical to the "diffraction minimum sharp" (dms) radius extracted from the minima of the electron scattering form factor. Moreover, as Friedrich and Voegler<sup>25</sup> have shown, this dms radius agrees well with the droplet model radius.<sup>27</sup>

In contrast to the experimentally observed variation of the rms radii, the proton radii predicted by

the droplet model increase monotonically with increasing atomic number, indeed in agreement with experimental rms radii of the even Ca isotopes. Consequently the experimental variation of the ms charge radii<sup>25</sup>

$$\delta \langle r^2 \rangle = \frac{3}{5} \delta R^2 + 3\delta \sigma^2 \quad (4.4)$$

is projected into a “shell effect” of the surface thickness  $\sigma$ . Figure 6 displays the variation of the diffuseness parameter  $a$  as required by the experimental  $\delta \langle r^2 \rangle$  values when combined with the droplet model predictions for  $\delta R^2$  [for calculating  $R$ , we used the parameter set recommended in Ref. 25 and  $a(^{40}\text{Ca})=0.566$ ]. As the ms deformation is contributing to the surface diffuseness, we define a reduced skin thickness  $\sigma$  by

$$\delta \langle r^2 \rangle = \frac{3}{5} \delta R^2 + 3\delta \bar{\sigma}^2 + \frac{5}{4\pi} \left( \frac{3}{5} R^2 + 3\bar{\sigma}^2 \right) \delta \langle \beta_L^2 \rangle. \quad (4.5)$$

The trend of the reduced diffuseness parameters of the even isotopes is also shown in Fig. 6. Obviously the difference in the ms octupole deformation [extracted from known  $B(E3;0^+ \rightarrow 3_1^-)$  values<sup>23</sup>] is able to explain the diffuseness difference of the two magic nuclei  $^{40}\text{Ca}$  and  $^{48}\text{Ca}$ . It is interesting to note that after such a deformation correction  $^{48,40}\delta \langle r^2 \rangle^{\text{corr}}$  is in excellent agreement with the droplet model. However, though the results do reveal the distinct influence of long range correlations

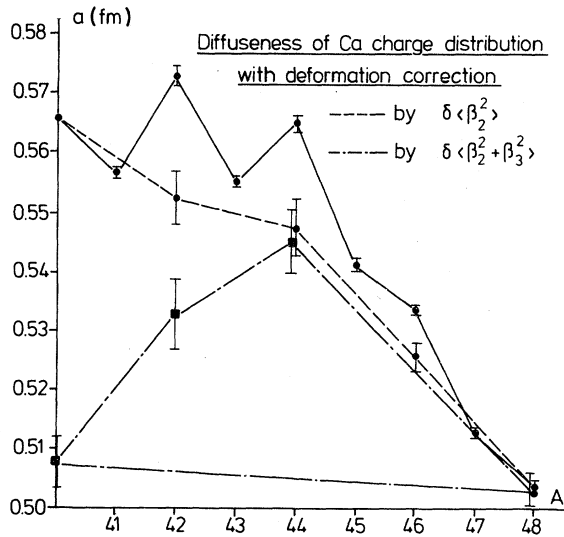


FIG. 6. Variation of the diffuseness parameter of a Fermi distribution as required by the measured  $\delta \langle r^2 \rangle$  values, with and without (full curve) ms deformation correction.

on the surface diffuseness, the remaining background diffuseness shows the same parabolic trend as seen for the ms radii and appears to be the true and unexplained origin of the observed radius variation.

The outstanding features of the Ca nuclei have also been the subject of various theoretical approaches based on a microscopic description of nuclear structure.<sup>28,29</sup> The overall trend in  $\delta \langle r^2 \rangle$  can be fairly well reproduced.<sup>28</sup> The superimposed odd-even staggering, which has been ascribed to a blocking of ground state correlations by the unpaired neutron<sup>30</sup> has been considered by Caurier *et al.*<sup>31</sup> in the framework of the isospin projected Hartree-Fock procedure. Configuration mixing is qualitatively able to explain the odd-even staggering, but inclusion of a larger number of orbitals becomes rapidly intractable.

In order to retain the essential physical features, Talmi<sup>32</sup> has proposed a simple model mixing to the shell model states

$$|I_{\text{core}}=0 f_{7/2}^n(I_0) I=I_0\rangle,$$

some other excited states

$$|I_{\text{core}}=2 f_{7/2}^n(I_1) I=I_0\rangle$$

( $f_{7/2}^n$  configurations coupled to an excited, presumably deformed<sup>36</sup> core state). Assuming that the mixing amplitudes do not depend on more detailed structure effects, a most simple expression is obtained

$${}_{40+n,40}\delta \langle r^2 \rangle = \begin{cases} K \times n(8-n) & \text{even } A \\ K \times [n(8-n)-4] & \text{odd } A \end{cases} \quad (4.6)$$

The parameter  $K$  includes the mixing amplitudes or nuclear matrix elements (expressing the  $n$  particle intraorbit interactions in terms of two-particle interactions). Formula (4.6) is related to a slightly more general expression<sup>33,34</sup> (originally given for the variation of the binding energies) with three parameters, which are, however, basically not independent and determined by the same matrix element. Even if such a simplified description (with  $K$  as an adjustable parameter) is not expected to fit the data extremely well (Fig. 7), it is impressive how clearly the general features of the experimental results are reproduced.

In addition to charge radii differences, electromagnetic moments provide further nuclear structure information and critical tests of microscopic theories. The experimental values of the magnetic moments of the odd isotopes (Table III) agree fairly well with theoretical results.<sup>29,37</sup> Using the operator

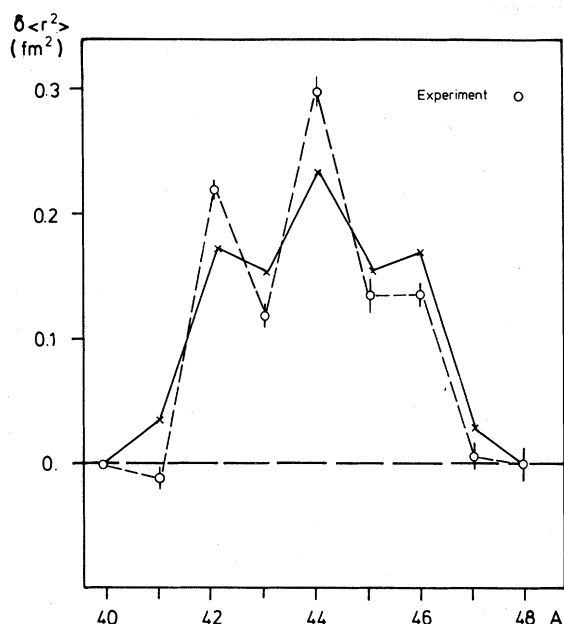


FIG. 7. Variation of the Ca charge radii in Talmi's model.

for the free nucleon (i.e., single particle dipole moments  $\mu_p = 2.79 \mu_N$  and  $\mu_n = -1.95 \mu_N$  for protons and neutrons, respectively) for  $^{47}\text{Ca}$ , a theoretical value  $\mu = -1.38 \mu_N$  is quoted.<sup>29</sup> The trend of the measured  $B$  factors confirms the change of the sign of the nuclear quadrupole moments in the middle of the shell as expected by shell model considerations.<sup>38,29</sup> As mentioned above (Sec. III B), a first order evaluation of the measured  $B$  factors would yield a value of the spectroscopic quadrupole moment of  $^{45}\text{Ca}$  which disagrees with previous experimental results,<sup>4</sup> but within the common uncertainty all first order results are not inconsistent with recent shell model calculations.<sup>29</sup>

#### ACKNOWLEDGMENTS

It is a pleasure to acknowledge stimulating and clarifying discussions with Prof. P. Brix, Prof. J. Friedrich, Prof. I. Talmi, and Prof. H. Walther. We thank Mr. B. Feurer for able technical assistance in preparing the Ca samples.

<sup>1</sup>Proceedings of the Karlsruhe International Discussion Meeting, 1979, edited by H. Rebel, H. J. Gils, and G. Schatz, Kernforschungszentrum Karlsruhe Report KfK 2830, 1979.

<sup>2</sup>H. Rebel, Institute of Physics Conference "Trends in Nuclear Structure Physics," University of Manchester, 1980, Kernforschungszentrum Karlsruhe Report KfK 2974, 1980.

<sup>3</sup>F. Träger, Z. Phys. A **299**, 33 (1981).

<sup>4</sup>E. Bergmann, P. Bopp, Ch. Dorsch, J. Kowalski, F. Träger, and G. zu Putlitz, Z. Phys. A **294**, 319 (1980); R. Neumann, F. Träger, J. Kowalski, and G. zu Putlitz, *ibid.* **279**, 249 (1976); U. Klingbeil, J. Kowalski, F. Träger, H. B. Wiegemann, and G. zu Putlitz, *ibid.* **290**, 143 (1979); J. Kowalski, F. Träger, S. Weisshaar, H. B. Wiegemann, and G. zu Putlitz, *ibid.* **290**, 345 (1979).

<sup>5</sup>A. Andl, K. Bekk, S. Göring, A. Hanser, G. Nowicki, H. Rebel, G. Schatz, and R. C. Thompson, European Conference on Atomic Physics, Heidelberg, 1981, Abstracts 5A, I, p. 200.

<sup>6</sup>A. Andl, Kernforschungszentrum Karlsruhe Report KfK 3191, 1981.

<sup>7</sup>H. Wohlfahrt, E. Shera, M. Hoehn, Y. Yamazaki, G. Fricke, and R. Steffen, Phys. Lett. **73B**, 131 (1978).

<sup>8</sup>G. Olsson and S. Salomonson, European Conference on Atomic Physics, Heidelberg, 1981, Abstracts 5A, I, p. 202; J. Bauche, G. Couarazze, and J. J. Labarth, Z. Phys. **270**, 311 (1974).

<sup>9</sup>G. Nowicki, K. Bekk, S. Göring, A. Hanser, H. Rebel, and G. Schatz, Phys. Rev. Lett. **39**, 332 (1977); Phys. Rev. C **18**, 2369 (1978).

<sup>10</sup>K. Bekk, A. Andl, S. Göring, A. Hanser, G. Nowicki, H. Rebel, and G. Schatz, Z. Phys. A **291**, 219 (1979).

<sup>11</sup>H. Fabricius, K. Freitag, S. Göring, A. Hanser, and H.-J. Langmann, Kernforschungszentrum Karlsruhe Report KfK 511, 1966.

<sup>12</sup>H. W. Brandt, K. Heilig, H. Knöckel, and A. Steudel, Z. Phys. A **288**, 241 (1978).

<sup>13</sup>K. Heilig and A. Steudel, At. Data Nucl. Data Tables **14**, 613 (1974).

<sup>14</sup>H. J. Kluge and H. Sauter, Z. Phys. **270**, 293 (1974).

<sup>15</sup>G. zu Putlitz, Ergeb. Exakten Naturwiss. **37**, 106 (1965).

<sup>16</sup>R. M. Sternheimer and R. F. Peierls, Phys. Rev. A **3**, 871 (1971).

<sup>17</sup>M. Arnold, J. Kowalski, T. Stehlin, F. Träger, and G. zu Putlitz, European Conference on Atomic Physics, Heidelberg, 1981, Abstracts 5A, II, p. 1107.

<sup>18</sup>P. Grundevik, M. Gustavsson, I. Lindgren, G. Olsson, L. Robertsson, A. Rosen, and S. Svanberg, Phys. Rev. Lett. **42**, 1528 (1979).

<sup>19</sup>R. Aydin, W. Ertmer, and U. Johann, Z. Phys. A **306**, 1 (1982).

<sup>20</sup>M. J. A. De Voigt, D. Cline, and R. N. Horoshko, Phys. Rev. C **10**, 1798 (1974).

<sup>21</sup>H. D. Gräf, M. Feldmeier, P. Manakos, A. Richter, and E. Spamer, Nucl. Phys. **A295**, 319 (1978).

- <sup>22</sup>P. M. Endt, *At. Data Nucl. Data Tables* **23**, 547 (1979).
- <sup>23</sup>A. Bernstein, in *Advances in Nuclear Physics*, edited by M. Baranger and E. Vogt (Plenum, New York, 1969), Vol. 3, p. 325.
- <sup>24</sup>P. G. Reinhard and D. Drechsel, *Z. Phys. A* **290**, 85 (1979).
- <sup>25</sup>J. Friedrich and N. Voegler, *Nucl. Phys.* **A373**, 192 (1982).
- <sup>26</sup>H. Überall, *Electron Scattering from Complex Nuclei* (Academic, New York, 1971).
- <sup>27</sup>W. D. Myers and W. J. Swiatecki, *Ann. Phys. (N.Y.)* **55**, 395 (1969); W. D. Myers, *Droplet Model of Atomic Nuclei* (Plenum, New York, 1977).
- <sup>28</sup>B. A. Brown, S. E. Massen, and P. E. Hodgson, *J. Phys. G* **5**, 1655 (1979).
- <sup>29</sup>B. J. Cole, *J. Phys. G* **7**, 25 (1981).
- <sup>30</sup>B. S. Reehal and R. A. Sorensen, *Nucl. Phys.* **A161**, 385 (1971).
- <sup>31</sup>E. Caurier, A. Poves, and A. Zuker, *Phys. Lett.* **96B**, 15 (1980).
- <sup>32</sup>I. Talmi, private communication.
- <sup>33</sup>I. Talmi, *Rev. Mod. Phys.* **34**, 704 (1962).
- <sup>34</sup>L. Zamick, Proceedings of the BANFF Conference on Nuclear Structure, Alberta, Canada, 1978 (unpublished).
- <sup>35</sup>G. W. Greenlees, D. L. Clark, S. L. Kaufmann, D. A. Lewis, J. F. Tonn, and J. M. Broadhurst, *Opt. Commun.* **23**, 236 (1977).
- <sup>36</sup>C. W. Towsley, D. Cline, and R. N. Horoshko, *Nucl. Phys.* **A204**, 574 (1973).
- <sup>37</sup>I. B. McGrory, *Phys. Rev. C* **8**, 93 (1973).
- <sup>38</sup>W. Kutschera, B. A. Brown, and K. Ogawa, *Rev. Nuovo Cimento* **1**, No. 12, 1 (1978).